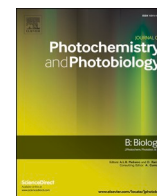




Contents lists available at ScienceDirect

## Journal of Photochemistry &amp; Photobiology, B: Biology

journal homepage: [www.elsevier.com/locate/jphotobiol](http://www.elsevier.com/locate/jphotobiol)

# *In vitro* 5-Fluorouracil resistance produces enhanced photodynamic therapy damage in SCC and tumor resistance in BCC

Jimena Nicolás-Morala<sup>a,b,1</sup>, Mikel Portillo-Esnaola<sup>a,b,1</sup>, Samuel Terrén<sup>a</sup>, María Gutiérrez-Pérez<sup>a</sup>, Yolanda Gilaberte<sup>c,\*</sup>, Salvador González<sup>b,d,1,\*</sup>, Ángeles Juarranz<sup>a,b,1,\*</sup>

<sup>a</sup> Department of Biology, Faculty of Sciences, Autónoma University of Madrid (UAM), Madrid 28049, Spain

<sup>b</sup> Instituto Ramón y Cajal de Investigación Sanitaria (IRYCIS), Madrid 28034, Spain

<sup>c</sup> Dermatology service, Hospital Miguel Servet, Zaragoza 50009, Spain

<sup>d</sup> Department of Medicine and Medical Specialties, Alcalá de Henares University, 28805 Madrid, Spain

## ARTICLE INFO

## Keywords:

Non-melanoma skin cancer  
5-Fluorouracil  
Tumor resistance  
Photodynamic therapy  
Protoporphyrin IX

## ABSTRACT

Non-melanoma skin cancer (NMSC) is the most common malignancy worldwide, with rising incidence in the recent years. It includes basal cell carcinoma (BCC), and squamous cell carcinoma (SCC). Several non-invasive therapies have been developed for its treatment such as topical 5-Fluorouracil (5FU) and photodynamic therapy (PDT), among others. Despite both are appropriated for NMSC treatment, recurrence cases have been reported. To prevent this, in this work we explore the potential of the combination of PDT and 5FU to treat SCC and BCC. First we evaluate the efficacy of PDT in cells resistant to 5FU. For this purpose, we use SCC-13 and CSZ-1 cells, obtained from a human SCC and a murine BCC, respectively. We first induced 5FU resistance in these cell lines by repeated treatments with the drug and then, the efficacy to PDT was evaluated. The results obtained indicated that SCC-5FU resistant cells were sensible to PDT administration, whereas BCC-5FU resistant cells were also resistant to PDT. The observed responses in both cell lines are in concordance to Protoporphyrin IX (PpIX) and reactive oxygen species (ROS) levels produced after the incubation with MAL and subsequent light exposure. The obtained data support the fact that PDT seems to be an appropriate therapeutic option to be administered after 5FU resistance in SCC. However, PDT would not be a choice therapy for resistant BCC cells to 5FU.

## 1. Introduction

Non-melanoma skin cancer (NMSC) is the most common malignancy among the Caucasian population, and its incidence has been increasing in recent decades. NMSC comprises basal cell carcinoma (BCC), and squamous cell carcinoma (SCC) [1]. Invasive therapies for NMSC include tangential shave removal, curettage, electrodesiccation, Mohs micrographic surgery and standard surgical excision. Nevertheless, non-invasive therapies such as topical 5-Fluorouracil (5FU), diclofenac,

cryotherapy, photodynamic therapy (PDT), laser therapy, immunotherapy, and radiotherapy usually offer better cosmetic outcomes [2].

The use of 5FU has substantially increased in the last years as therapy for actinic keratosis (AK, a premalignant situation of SCC), *in situ* SCC and superficial BCC since its approval by the European Medicines Agency (EMA) and the Food and Drug Administration (FDA) [3]. 5FU is a chemotherapeutic drug which mainly acts interfering with DNA synthesis through the inhibition of the enzyme thymidylate synthase, causing cell cycle arrest and tumor cell death. Besides, 5FU interferes

**Abbreviations:** NMSC, Non-melanoma skin cancer; BCC, Basal cell carcinoma; SCC, Squamous cell carcinoma; 5FU, 5-Fluorouracil; PDT, Photodynamic therapy; AK, Actinic keratosis; ROS, Reactive oxygen species; PpIX, Protoporphyrin IX; ALA,  $\delta$ -Amino-levulinic acid; MAL, Methyl-aminolevulinate; EMT, Epithelial-mesenchymal transition; FBS, Fetal Bovine Serum; PBS, Phosphate-buffered saline; IF, Indirect Immunofluorescence; HO-1, Heme oxygenase-1; DCFH-DA, Dichlorodihydro-fluorescein diacetate; ANOVA, Analysis of variance.

\* Corresponding authors at: Department of Biology, Faculty of Sciences, Universidad Autónoma de Madrid, 28049, Madrid, Spain and Instituto Ramón y Cajal de Investigación Sanitaria (IRYCIS), Madrid, 28034, Spain.

\*\* Correspondence to: Dermatology Service, Hospital Miguel Servet, Zaragoza, 50009, Spain.

E-mail addresses: [jimena.nicolas@uam.es](mailto:jimena.nicolas@uam.es) (J. Nicolás-Morala), [ygilaberte@gmail.com](mailto:ygilaberte@gmail.com) (Y. Gilaberte), [salvagonrod@gmail.com](mailto:salvagonrod@gmail.com) (S. González), [angeles.juarranz@uam.es](mailto:angeles.juarranz@uam.es) (Á. Juarranz).

<sup>1</sup> Authors contributed equally to this work.

<https://doi.org/10.1016/j.jphotobiol.2022.112483>

Received 12 February 2022; Received in revised form 10 May 2022; Accepted 25 May 2022

Available online 29 May 2022

1011-1344/© 2022 The Author(s). Published by Elsevier B.V. This is an open access article under the CC BY-NC-ND license (<http://creativecommons.org/licenses/by-nc-nd/4.0/>).

with RNA synthesis being transformed within the cell to an analogous of uridine triphosphate [4]. 5FU has been demonstrated to be very efficient in AK and *in situ* SCC, with up to 96% of effectiveness 4 weeks after its administration [5], alongside superficial BCC, with a 90–93% of tumor clearance after treatment finalization [6].

PDT has shown to be an excellent treatment option for these skin processes [7]. PDT consists in the administration of a photosensitizer (PS), which accumulates preferentially in tumor cells followed by its activation upon exposure to adequate wavelength light. In NMSC red light is usually used due to its higher tissue penetrance. The activation of the PS triggers the production of reactive oxygen species (ROS), causing cell damage and the consequent cell death. Protoporphyrin IX (PpIX) is an endogenous PS and intermediate metabolite in the heme biosynthesis.  $\delta$ -Amino-levulinic acid (ALA) and its methyl derivative methyl-aminolevulinate (MAL), which are precursors of the photoactive PpIX, are frequently used for PDT in NMSC. PpIX accumulation is higher in tumor tissues mainly due to specific alterations on several enzymes of the heme biosynthesis pathway in these cells [8,9]. Under physiological conditions PpIX is transformed into heme by the enzyme ferrochelatase, however, in tumor cells the activity of this enzyme is substantially impaired [10], leading to the accumulation of the PS. This abnormal PpIX accumulation is even higher when ALA or MAL are exogenously administered leading to damage and subsequent death of tumor cells after light exposure. Overall, PDT presents very promising results, with resolution rates ranging from 90 to 100% in different subtypes of NMSC at 6-month follow-up, with excellent cosmetic outcomes. [11,12]

Although both PDT and 5FU treatments present promising short-term outcomes, long-term studies reported high recurrence rates. In SCC, a study reported recurrence rates up to 15% after MAL-PDT and 17% in the 5FU group 12 months after treatment finalization [13]. In BCC, 5-year recurrence rates ascend to 21% for 5FU after the treatment [7] and 30% after PDT [11], making therapy resistance a major problem for complete tumor eradication. Although many studies have focused on cancer resistance to drugs and the subjacent mechanisms of this resistance process, very few are aimed to NMSC.

As previously indicated, 5FU acts by interfering with DNA synthesis. However, some cells develop the capacity to adapt their mechanisms to overcome the effects of this drug, promoting tumor survival and potential residual tumor cells. Different 5FU-resistant cell lines have shown cell cycle arrest in G1/S leading to cell damage avoidance by slowing down DNA synthesis and improving repair mechanisms [14]. Regarding epithelial-mesenchymal transition (EMT), 5FU-resistant cells express low levels of epithelial markers such as E-cadherin but high levels of mesenchymal markers such as vimentin [14]. Lastly, different alterations in the Notch pathway have been reported, which confer 5FU resistance through EMT promotion and overexpression of transporters from the ABC family [15].

Several combinations of different therapies are being developed as potential solutions to prevent recurrences in NMSC. In this regard, encouraging results have been obtained when PDT is combined with other available therapies. For instance, in AK, combinations of PDT with imiquimod (an immunomodulatory drug which bind toll-like receptors and promotes apoptosis), radiotherapy or different lasers, have resulted in increased efficacy [16]. Furthermore, several studies have proven increased efficacy of ALA-PDT with a 5FU pre-treatment *in vitro* in A431 cells, a vulvar SCC cell line [17], and in AK in clinical trials [18]. Surprisingly, this combination was ineffective in BCC patients, causing an antagonistic effect and severe damage including ulceration and redness [19].

Taking these previous results into account, we developed two 5FU resistant cell lines with the objective of studying whether the acquisition of 5FU resistance influences the PDT response in the same way the combination with 5FU did. The first cell line comes from a cutaneous SCC, SCC-13 (SCC13), and the second comes from a BCC, CSZ1 (CSZ). Both original cell lines, named as parental lines, underwent 10 cycles of 5FU, originating two 5FU resistant cell lines. These cell lines were

analysed and characterized and their response to PDT was evaluated afterwards. The results showed that the SCC 5FU resistant cells presented increased PDT sensitivity, while BCC 5FU resistant cells showed increased resistance to this therapy. These results open the possibility to consider PDT as an adequate therapy as a second line treatment in 5FU resistant SCC cells. In contrast, that would not be beneficial in case of 5FU resistant BCC cells.

## 2. Materials & Methods

### 2.1. Cell Lines and Culture

Two established cell lines of NMSC, SCC13 cells from a human cutaneous facial SCC [20], and CSZ cells from a mouse BCC (*pth* +/–) [21] were employed. The original cells were named as parental cells (SCC13 P and CSZ P) and the resistant cells generated after 10 cycles of 5FU were named as SCC13 10G 5FU and CSZ 10G 5FU. The cell line A431 [17] from a vulvar SCC was used as control for therapy combination. All cell lines were grown in complete medium Dulbecco's Modified Eagle's Medium (DMEM) supplemented with 10% Fetal Bovine Serum (FBS) and 1% Penicillin-Streptomycin. Cells were incubated in a CO<sub>2</sub> incubator with a temperature of 37 °C, 5% CO<sub>2</sub> and 95% humidity. For the development of 2D experiments, cells were grown in monolayer within multi-well plates to a 30% confluence and given treatments afterwards.

### 2.2. Treatments

For PDT treatment, SCC13 and CSZ cells were grown on multi-well plates to a 60% confluence, 72 h after seeding. Then, cells were incubated with MAL (*Sigma*) at a concentration of 0.6 mM in the case of SCC13 and A431 cells and at 0.3 mM in the case of CSZ cells. MAL was administered in DMEM without FBS for 5 h of incubation. All the conditions had been successfully established in our laboratory. Administration of MAL was carried out in the absence of FBS because cytokines present on it could influence the response to the therapy. [22,23]. Then, the cells were irradiated with red light (635 nm) by using a LED irradiator (laboratory designed, *Segainvex*, *UAM*) formed by 384 light emission diodes irradiating at 10.2 mW/cm<sup>2</sup>. Different doses of red light ranging from 0.6 J/cm<sup>2</sup> to 12 J/cm<sup>2</sup> were used. After irradiation, culture medium was replaced with fresh DMEM containing 10% FBS and cells were kept in the CO<sub>2</sub> incubator until evaluation, 24 h after the irradiation.

For the treatment with 5FU, SCC13 and CSZ cells were treated for 72 h with 5FU at different concentrations (ranging from 10 nM to 1000 nM). After 5FU treatment, cells were washed three times with PBS and later evaluated.

To perform the combined treatment 5FU plus PDT, cells were grown to a 30% confluence and a 48 h pre-treatment of 5FU (*Sigma*). The administered 5FU doses were 100 nM in SCC13, 200 nM in CSZ and 400 nM in A431, which represented an approximate lethal dose of 50% (LD50). Just after finishing 5FU incubation, cells were incubated with MAL at the indicated conditions, washed in PBS and exposed to variable red-light doses. Evaluation was performed 24 h after the combined treatment. The cells treated only with 5FU were not incubated with MAL but exposed to red light (not detrimental).

### 2.3. Development of 5FU Resistant Cell Lines

To obtain resistant cells to 5FU, cells were grown to a 40% of confluence in a 25 cm<sup>2</sup> area flask and were incubated with 10  $\mu$ M 5FU for 72 h. Then, 5FU was properly removed and cells were washed with sterile phosphate-buffered saline (PBS) 1 $\times$  and replaced with complete culture medium to let the cells rest after the treatment until their total recovery. This process was repeated 10 times to generate the SCC13 10G 5FU and CSZ 10G 5FU cell lines (Fig. S1).

## 2.4. Spheroids Formation

Spheroid formation was carried out by suspending 20.000 cells/ml of SCC13 and CSZ, parentals and resistant cells, in a specific culture medium [24]. This medium was composed by DMEM:F12 (1:1) supplemented with 20 ng/ml of EGF (*Sigma*), 4 µg/ml insulin (*Sigma*) and 2% of B27 supplement (*Invitrogen*). The cell suspension was seeded in six-well plates coated with 1.2% poly-HEMA (2-hydroxyethyl methacrylate, *Sigma*) in ethanol 96%, in agitation at 65 °C. 2.5 ml of the solution was placed in each well and the ethanol was let to evaporate overnight and sterilized with 1 h of UV irradiation before seeding the cells. The spheroids were grown for 5 days to be completely formed.

## 2.5. Cell Viability Evaluation

After the treatments, cell viability of the monolayer cultures was evaluated by using the MTT (3-(4,5-dimethylthiazol-2-yl)-2,5-diphenylthiazole bromide, *Sigma*) assay [25]. For this purpose, after the different treatments, cells were incubated with 100 µg/ml of MTT in complete medium for 3 h. After that, formazan crystals were solubilized with dimethyl sulfoxide to be measured through spectrophotometry at 542 nm with a Tecan SPECTRAFluor Plus Microplate Reader.

In the case of the spheroids, the viability was evaluated by using the Acridine Orange/Propidium Iodide (*ThermoFisher*) test. Both fluorochromes were added directly to the wells containing the spheroids at a concentration of 50 µg/m. Photographs were taken by using fluorescence microscopy with blue ( $\lambda = 450\text{--}490$  nm) and green light excitation ( $\lambda = 590$  nm). All cells were stained with Acridine Orange fluorescence and visualized under green filter. Dead cells were stained by Propidium Iodide and emitted red fluorescence. The viability of spheroids was measured dividing the integrated density of dead cells by the integrated density of the total of the spheroid. Integrated density value of each spheroid is obtained with the program Image J.

## 2.6. Indirect Immunofluorescence

Indirect Immunofluorescence (IF) was performed on SCC13 and CSZ cells grown on coverslips. Once they reached the 50–70% confluence, cells were fixed in formaldehyde 3,7% in PBS during 30 min at 4 °C. Afterwards, cells were properly washed with PBS, permeabilized with 0.1% Triton X100 in PBS, and incubated with the antibodies for Heme oxygenase-1 (HO-1, *Cell Signalling Technology*) in a 1:100 dilution for 1 h at 37 °C. Then, cells were washed with PBS and incubated with the corresponding secondary antibody (Goat anti-rabbit Alexa Fluor 546, *Invitrogen*, respectively) in a 1:250 dilution for 45 min at 37 °C. Both antibodies were diluted in PBS/BSA 0.5%. After washing, the cells were counterstained with Hoechst-33,258 (1 µg/ml, *Sigma*) for 5 min, washed again in PBS and coverslips mounted on a slide using Prolong (*Life Technologies*). In order to identify dividing cells, cells were only stained with Hoechst-33,258 (1 µg/ml, *Sigma*) after fixation.

## 2.7. PpIX Production

To measure the production of PpIX, cells were incubated for 5 h with MAL 0.6 mM (SCC13) or 0.3 mM (CSZ), setting the previous performed conditions. After that, cells were trypsinized and centrifuged at 1600 rpm for 7 min, fixed in 1% formaldehyde at room temperature and washed two times with PBS. The samples were kept overnight in the dark and, PpIX was measured in the cells in suspension by flow cytometry (FC500 Cytomics 2 *Beckman lasers*) using a  $\lambda = 625$  nm for excitation and a  $\lambda = 670$  nm for emission. Production of PpIX was also checked under the fluorescence microscope. For that, cells were grown on coverslips, incubated with MAL for 24 h and directly observed the red fluorescence, due to PpIX production, under green light excitation

## 2.8. ROS Generation

ROS production was determined under the fluorescence microscope. For that, cells were grown on coverslips and incubated with 0.6 mM or 0.3 mM MAL for 5 h and irradiated with red light (635 nm) 6 J/cm<sup>2</sup>. One hour before fluorescence microscopy observation 7.5 µM of Dichlorodihydro-fluorescein diacetate (DCFH-DA, *Abcam*) was added to every well. After irradiation, cells were briefly washed with PBS and directly observed under blue exciting light. ROS were detected fluorescing in green.

## 2.9. Fluorescence Microscopy and Image Processing

Fluorescence microscopy observations were performed with an Olympus BX-61 fluorescence microscope. Filters sets: blue (450–490 nm, exciting filter BP 490), green (545 nm, exciting filter BP 545). Photographs were taken with a CCD DP70 Olympus camera. Treatment and processing of photographs was done with Photoshop CS5 (*Adobe Systems Inc.*, USA). The quantification of the fluorescence emission was measured using ImageJ version 1.52a (NIH, Bethesda, MD, USA).

## 2.10. Statistical Analysis

All experiments were performed at least three times. Statistical analyses were effectuated using GraphPad Prism (*GraphPad Software Inc.*, USA) 6.05 version. Statistical differences were analysed with one or two-way analysis of variance (ANOVA) and *post hoc* analysis with Bonferroni test setting significant differences with *p*-values <0.05. (\*: *p* < 0.05; \*\*: *p* < 0.01; \*\*\*: *p* < 0.001).

# 3. Results

## 3.1. Cell Survival Evaluation after PDT and 5FU Treatments

To establish the conditions for evaluating the effect of the combination of the two therapies (PDT and 5FU), first we determined the effects on cell survival of each therapy administered individually in SCC13 and CSZ cells. In addition, A431 cells were used as control of efficacy of the treatments since these cells had already been used in previous studies with successful outcomes in therapy combination [17] (Fig. S2).

Regarding 5FU treatment, both SCC13 P and CSZ P cell lines showed similar sensibilities to the therapy, where the chemotherapeutic compound induced a significant decrease in cell viability in all the concentrations used in the evaluation (Fig. 1A).

In the case of PDT, CSZ P cells showed a higher sensibility to the therapy compared to that of SCC13 cells, which exhibited a lower toxicity to the photo-treatment (Fig. 1B). According to these results, we selected the corresponding conditions for the rest of the experiments regarding the efficacy of combination of both therapies.

## 3.2. The Combination of 5FU + PDT Displayed a Synergistic Effect in SCC13 and an Antagonistic Effect in CSZ Cells

After evaluating the effects of the individualized treatments, we next analysed the combined treatments in both cell lines. As previously indicated, we selected the treatment conditions that induced an approximate LD50 of 5FU (100 nM in SCC13 and 200 nM in CSZ in combination with PDT (MAL and variable light doses).

In SCC13 P, 5FU and PDT induced significantly higher levels of cell death when combined compared to PDT or 5FU by themselves, as it is shown from the viability data obtained by the MTT test. This effect was observed at all light doses administered except for the lowest dose used in combination compared to 5FU alone (Fig. 2A). The effects of the combination of both therapies in SCC13 P were calculated through the difference of logarithms (DL) [26], and a synergistic effect between both therapies was observed at every dose of red light administered (Fig. 2B).

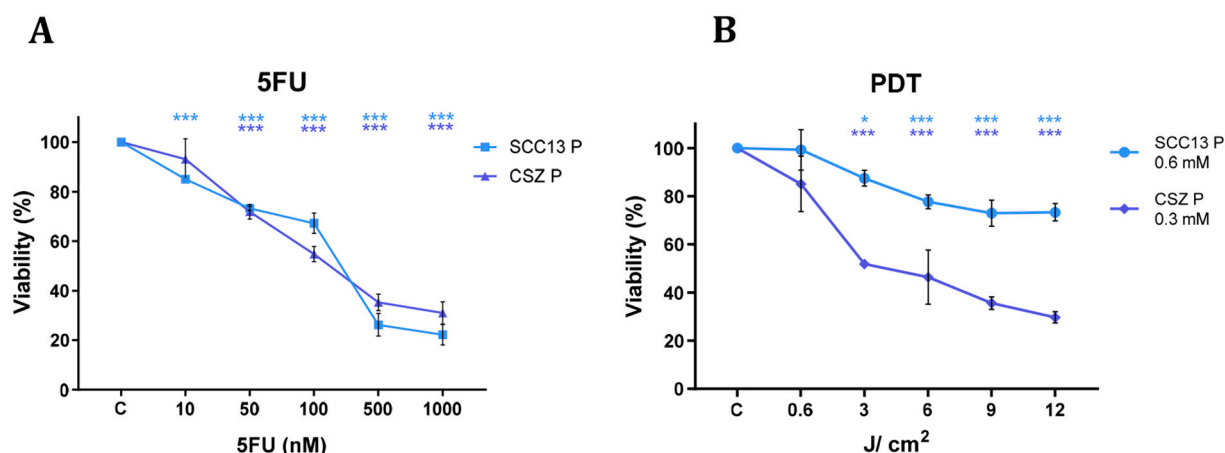


**Fig. 1. Measurement of cell survival after 5FU and PDT.** (A) The viability of SCC13 P and CSZ P cells was measured after 72 h of treatment with different 5FU concentrations. (B) The viability of SCC13 P and CSZ P cells was measured after 5 h incubation with 0.6 mM MAL (SCC13) or 0.3 mM MAL (CSZ) followed by exposure to different red-light doses. Cellular viability was determined by the MTT assay and expressed as the percentage of surviving cells relative to the non-treated (control) cells. \* means significant differences compared with the Control group (\*:  $p < 0.05$ ; \*\*:  $p < 0.01$ ; \*\*\*:  $p < 0.001$ ) ( $n = 3$ ). (For interpretation of the references to colour in this figure legend, the reader is referred to the web version of this article.)

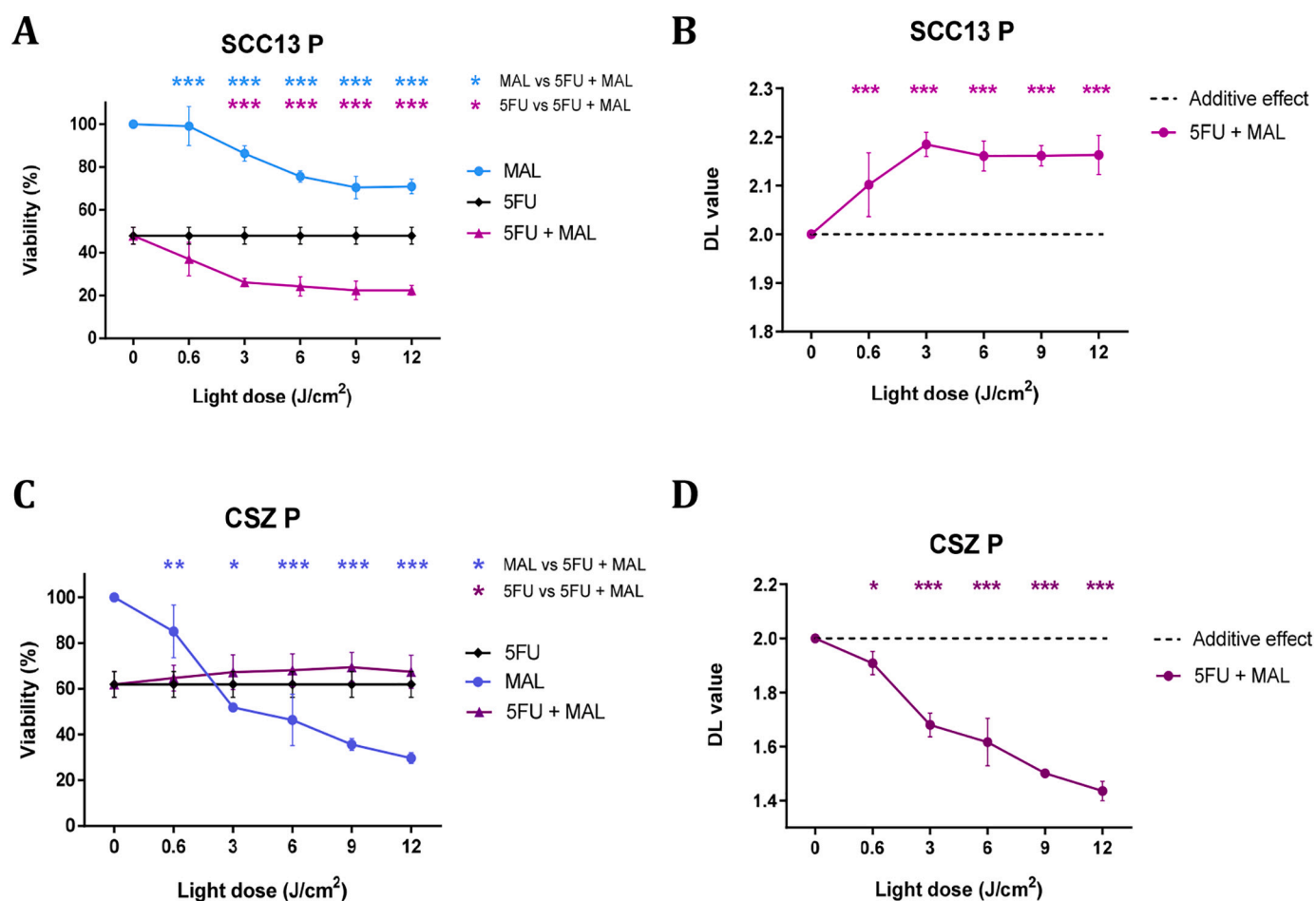


**Fig. 2. Evaluation of 5FU + PDT combination.** (A) SCC13 P viability after 5FU treatment, PDT and their combination. 100 nM 5FU was administered to the cultures for 48 h. For PDT, cells were incubated with 0.6 mM MAL for 5 h followed by exposure to different red-light doses. Cell viability was measured by the MTT assay (B) Synergistic effect of 5FU + PDT displayed by SCC13 P. A > 2 DL value with \* means significant synergistic effect. DL (difference of logarithms) = log SP additive – log SP combined [26]. (C) Viability of CSZ P after the administration of 5FU, PDT and their combination. 200 nM 5FU was applied for 48 h to the cells. After that, cells were incubated for 5 h with 0.3 mM MAL followed by red light exposure. (D) Effect of the combination of 5FU + PDT in CSZ P. A DL value below 2 with \* means significant antagonistic effect.  $n = 3$  (\*:  $p < 0.05$ ; \*\*:  $p < 0.01$ ; \*\*\*:  $p < 0.001$ ) ( $n = 3$ ). (For interpretation of the references to colour in this figure legend, the reader is referred to the web version of this article.)



CSZ P showed no significant differences in cell viability between the 5FU administrated alone and in combination with PDT, presenting only slightly higher, but not significant, values when both treatments were combined. The obtained DL values significantly below 2, indicated an antagonistic effect between both therapies in CSZ P (Fig. 2D).

Carrying the same experimental procedure in A431, we found out that those cells presented an increased cell death when 5FU + MAL-PDT was applied. In fact, an additive effect was seen since there was no significant differences between the obtained DL values and a 2 DL value that determines the presence of an additive effect (Fig. S3).

### 3.3. SCC13 10G 5FU and CSZ 10G 5FU Displayed Increased 5FU Resistance and Lower Proliferation Rates

We next obtained cell populations resistant to 5FU in order to evaluate the effects of the combined treatments in these types of cells. For that, cells were subjected to 10 cycles of 72 h of 5FU 10  $\mu$ M. After the repeated treatments, we confirmed the resistance of the resultant cell populations (10G 5FU). For that, by using the MTT test, we evaluated the effects of different 5FU concentrations for 72 h on cell viability. The results are shown in the Fig. 3. SCC13 10G 5FU cells displayed significantly higher viability compared to that of SCC13 P at every dose evaluated (Fig. 3A). CSZ 10G 5FU cells also showed higher viability rates after 5FU treatment when compared with CSZ P at the doses analysed

(Fig. 3B).

Once the induced resistance to 5FU was assessed, we analysed the proliferation rates of the parental and resistant cells by Hoechst staining. Dividing and non-dividing cells were counted to estimate the mitotic index and the mean  $\pm$  SEM was represented. Differences between the proliferation rates were observed between parental and resistant cells (Fig. 3C). The SCC13 P cell line displayed a mitotic index (MI) of  $2 \pm 0.34\%$  meanwhile that of SCC13 10G 5FU was of  $0.90 \pm 0.30\%$ . Regarding CSZ cell line, parental cells displayed a MI of  $4.40 \pm 0.62\%$ , in contrast, 10G 5FU resistant cells presented a lower MI of  $2.90 \pm 0.17\%$ . These results showed a significant decrease in the proliferation rate in both 5FU resistant lines, as compared to parental cells (Fig. 3D).

### 3.4. PpIX Production in SCC13 and CSZ Cells

To decipher the possible response to PDT that these cell lines would have, we assessed the production of PpIX in both, parental and resistant cells. Cells were incubated for 5 h with 0.6 mM (SCC13) and 0.3 (CSZ) mM MAL and PpIX production was evaluated by flow cytometry. PpIX production in SCC13 10G 5FU was significantly higher than that of SCC13 P. On the contrary, CSZ 10G 5FU displayed a significant lower PpIX levels compared to its parental line. No significant differences in the basal production of PpIX between SCC13 10G 5FU and SCC13 P were detected (Fig. 4A).

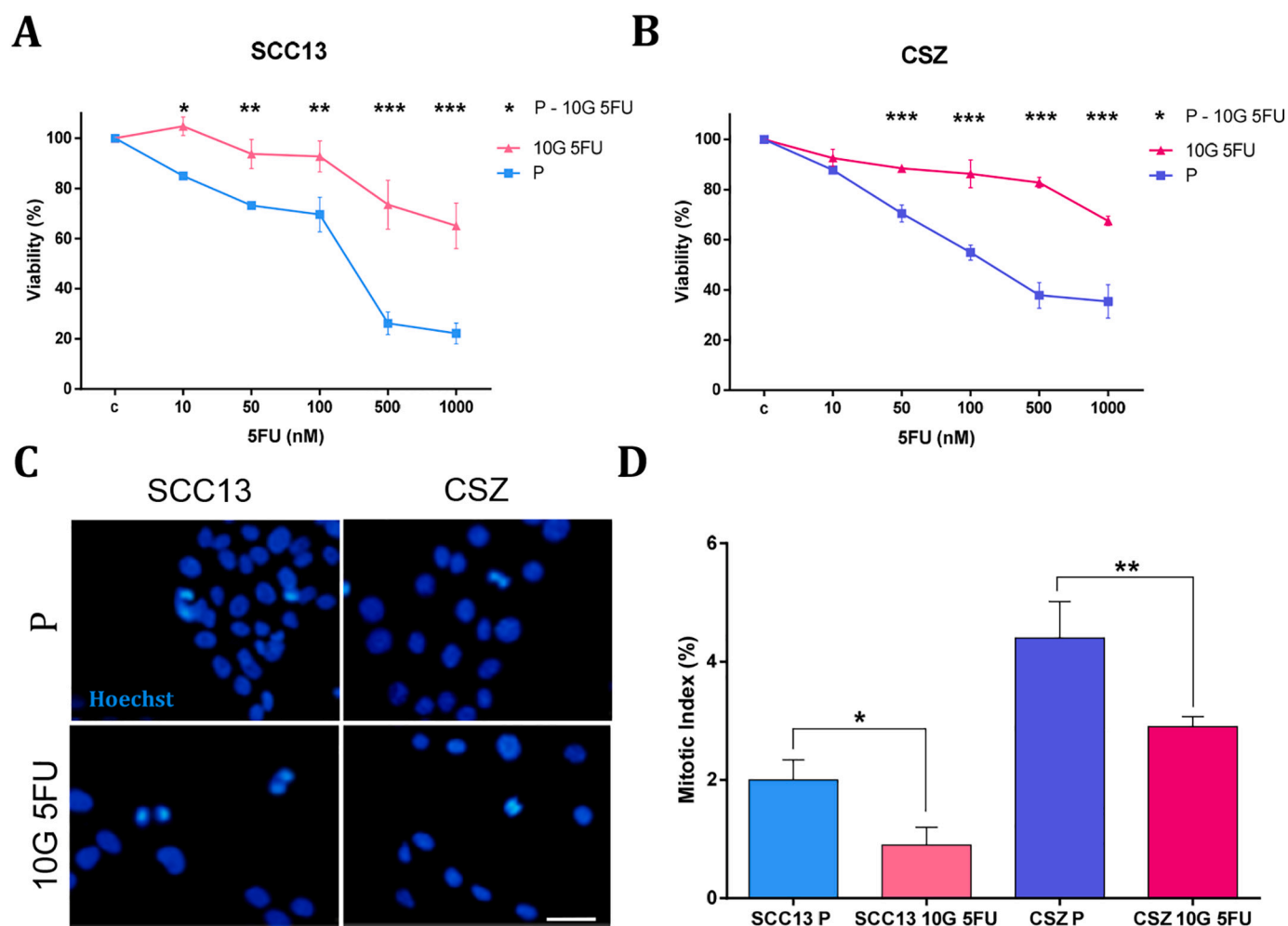


**Fig. 3.** Resistance measurement after 5FU treatment and Mitotic index estimation. (A) SCC13 cells viability after 72 h of treatment with different 5FU concentrations. (B) CSZ cells viability after 72 h of different 5FU concentrations. Cellular viability was measured by the MTT assay and expressed as the percentage of surviving treated cells relative to the non-treated (control) cells. (C) Dividing cells evaluated by Hoechst staining. Scale bar: 50  $\mu$ m (D) Comparison analysis of MI expressed in percentage for all cell lines; at least 1000 cells were counted for each condition (\*:  $p < 0.05$ ; \*\*:  $p < 0.01$ ; \*\*\*:  $p < 0.001$ ) ( $n = 3$ ).

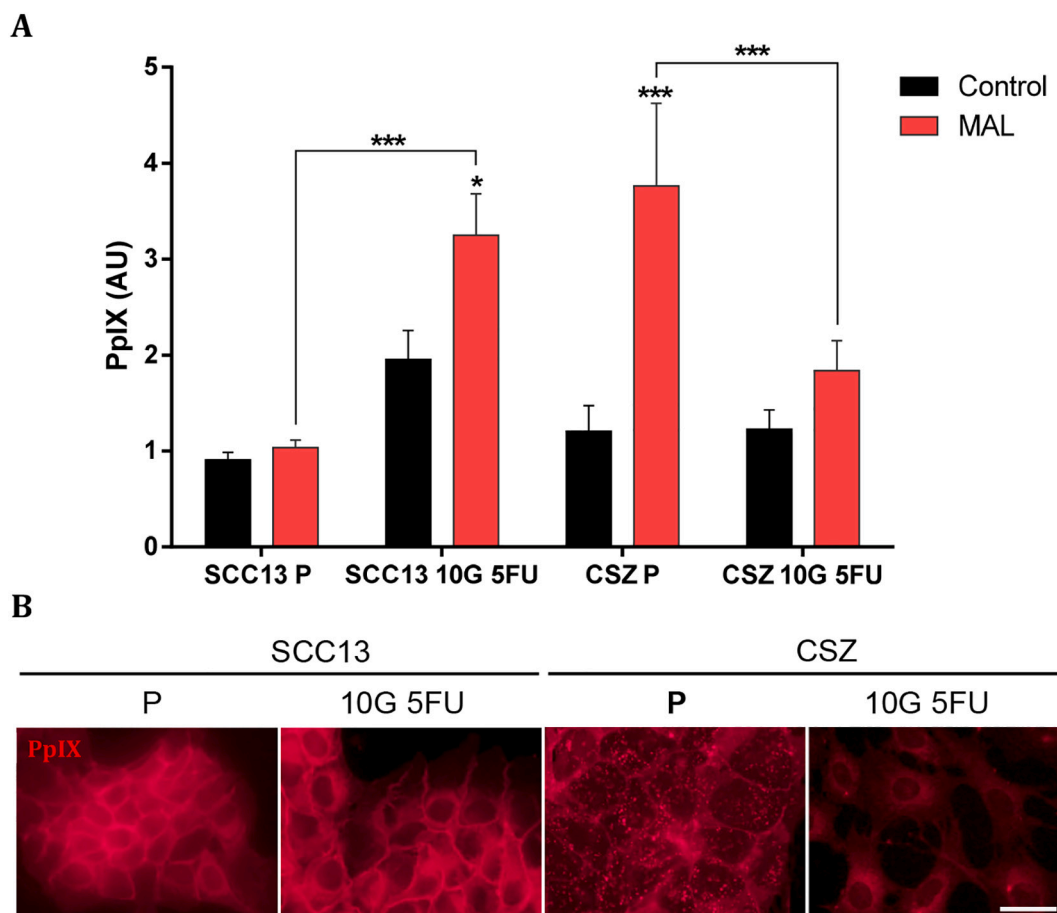


**Fig. 4. Production and localization of PpIX.** (A) PpIX production was evaluated by flow cytometry after cell incubation with MAL 0.6 mM (SCC13) or 0.3 mM (CSZ) for 5 h. Data were normalized to the basal values obtained in SCC13 P control. \* Indicates significant difference of PpIX production compared to its Control (not incubated with MAL) (\*:  $p < 0.05$ ; \*\*:  $p < 0.01$ ; \*\*\*:  $p < 0.001$ ) ( $n = 3$ ). (B) PpIX localization was performed after incubation with MAL at the indicated concentrations for 24 h. PpIX fluorescence was observed under the fluorescence microscopy by using exciting green light (590 DM filter). Scale bar 10  $\mu$ m. (For interpretation of the references to colour in this figure legend, the reader is referred to the web version of this article.)

In addition, we confirmed the production of PpIX under the fluorescence microscope. For that, SCC13 and CSZ cells (both, parental and resistant lines) were incubated with 0.6 mM (SCC13) and 0.3 mM MAL for 24 h and immediately visualized under exciting green light. PpIX fluorescence was observed in the cell membrane and around the cell nucleus in SCC13 P and SCC13 10G 5FU. However, in CSZ P, PpIX was distributed in the cell membrane and diffusely in the cytoplasm. In CSZ 10G 5FU, PpIX was located at perinuclear level, but not in cell membrane as CSZ P (Fig. 4B).

### 3.5. Differential ROS Levels between Parental and 5FU Resistant Cells

Considering the obtained results in PpIX production analysis, we checked the generation of ROS levels after PDT administration through DCFH-DA staining. ROS levels were minimal in the Control groups with practically no detected signal. When PDT was applied, both SCC13 cells (P and 10G 5FU) exhibited a heterogeneous pattern of ROS production, between cells within colonies, being higher in the borders of the colonies. In the case of CSZ cells, both populations (P and 10G 5FU) displayed a unified pattern of signal intensity due to ROS production (Fig. 5A and S4). Basal levels of ROS (cells not subjected to PDT) were similar in the four cell lines, with no significant differences between them. After PDT, SCC13 10G 5FU presented significantly higher levels of ROS, compared to its parental cell line. In BCC, CSZ 10G 5FU showed significantly lower fluorescence signal compared to CSZ P (Fig. 5B).

### 3.6. Response to PDT of SCC13 and CSZ Cells Resistant to 5FU

We next evaluated the response of the different cell lines to PDT in 2D and in 3D. SCC13 10G 5FU cells grown in monolayer displayed a higher sensibility to PDT than the parental SCC13 cells (Fig. 6A). On the contrary, CSZ P was more sensible to the PDT than the resistant CSZ 10G 5FU cells (Fig. 6B).

We also evaluated the response of these cell lines grown three-dimensionally (3D) forming spheroids. Once formed, spheroids were subjected to PDT. The original spherical shape was altered after PDT, inducing irregular morphologies. The viability was evaluated 24 h after the treatment with Acridine Orange/Propidium Iodide staining. In control conditions, only green signal given by Acridine Orange could be observed. However, after PDT a high red signal was observed due to internalization of propidium iodide in those cells undergoing cellular death (Propidium Iodide could penetrate due to changes in membrane permeability) (Fig. S5). SCC13 P spheroids suffered significantly less damage than those formed by SCC13 10G 5FU cells, which presented an increased damage facing the same PDT dose. On the opposite, CSZ P spheroids were significantly more damaged by PDT compared to those formed by CSZ 10G 5FU (Fig. 6C, D).

### 3.7. Heme Oxygenase-1 Levels in SCC13 and CSZ Cell Lines

The expression of the antioxidant molecule HO-1 is closely related to PDT resistance. This Nfr2-regulated gene codifies for an antioxidant

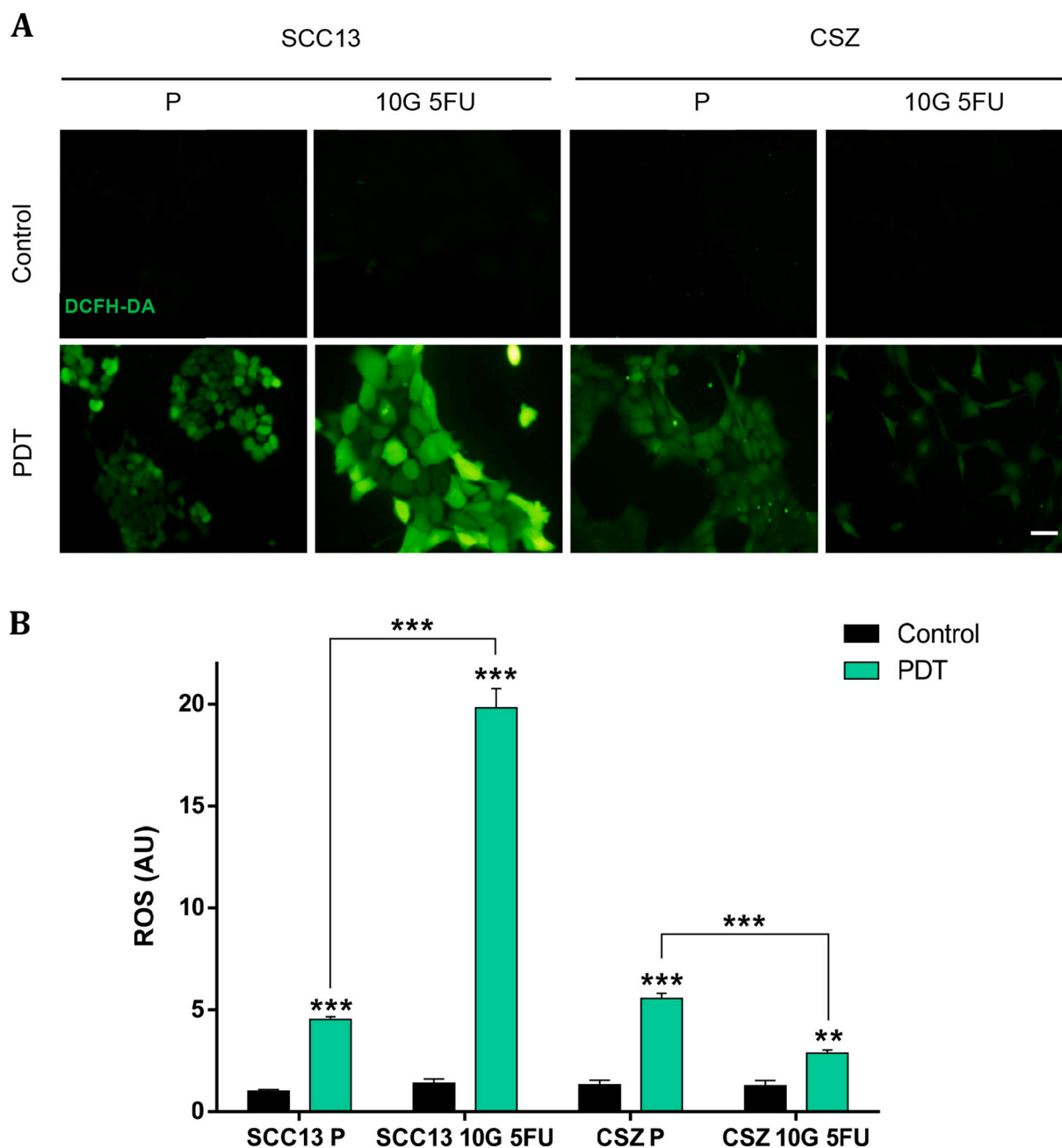


**Fig. 5. Measurement of basal and MAL-induced ROS production.** (A) ROS production (fluorescing in green) was detected by fluorescence microscopy under blue exciting light (490 BP filter) after PDT treatment: 5 h incubation with 0.6 (SCC13) mM or 0.3 mM (CSZ) MAL followed by 6 J/cm<sup>2</sup> of red-light exposure. Scale bar 10  $\mu$ m. (B) ROS determination was carried out by measuring the fluorescence mean of each condition and being normalized to SCC13 P Control (cells not subjected to PDT). \* Indicates significant differences of ROS production regarding its control condition (\*:  $p < 0.05$ ; \*\*:  $p < 0.01$ ; \*\*\*:  $p < 0.001$ ) ( $n = 3$ ). (For interpretation of the references to colour in this figure legend, the reader is referred to the web version of this article.)

molecule that counteracts the oxidative stress phenomenon induced by PDT [27]. Therefore, we decided to evaluate the expression of this enzyme in order to correlate it with the resistance to the therapies evaluated.

The IF revealed some differences between the used cell lines. SCC13 P cells presented a higher intense fluorescence signal, localized both in the cytoplasm and nucleus, meanwhile the nuclear fluorescence of the corresponding 5FU resistant population was very low and HO-1 was mostly located in the cytoplasm.

In CSZ, the opposite trend was observed where no fluorescence was detected in the nucleus in most parental cells, but some diffuse signal in the nuclei of CSZ 10G 5FU cells could be observed (Fig. 7A). In the

merged images a purple signal was detected in SCC13 P and CSZ 10G 5FU, corresponding with the nuclear HO-1 signal superimposed with blue Hoechst signal. Regarding intensity of the signal, significant differences in HO-1 expression was obtained: SCC13 P presented higher signal levels of HO-1 compared to its resistant line and, on the contrary, in the case of CSZ, the parental cell line displayed less intensity than the resistant one (Fig. 7B).

#### 4. Discussion

NMSC is the most prevalent cancer worldwide. Although it is not usually a very aggressive type of cancer (especially BCC), it represents a

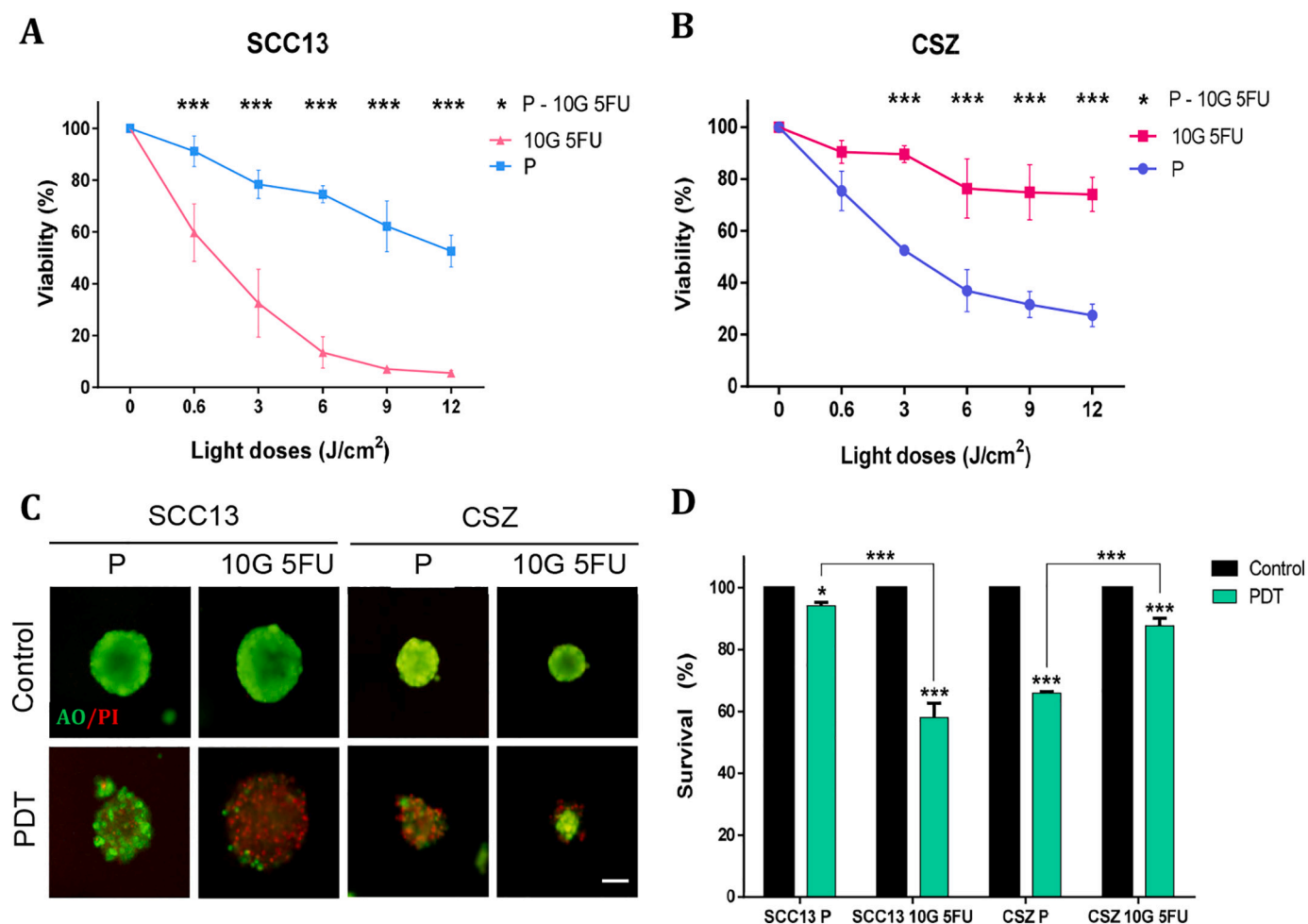


**Fig. 6. Response to PDT of 2D and 3D cultures of SCC13 and CSZ.** (A) SCC13 cells monolayer were subjected to PDT treatment (0.6 mM MAL and different red-light doses) and the effects of the treatment on cell viability was evaluated by MTT assay. (B) CSZ cells monolayer were subjected to PDT (0.3 mM MAL and different red-light doses) and the viability was also measured by the MTT assay. Cellular viability was expressed as the percentage of surviving cells relative to the non-treated (control) cells. (C) SCC13 and CSZ spheroids untreated and after PDT with 0.6 mM (SCC13) and 0.3 mM of MAL (CSZ) followed by 6 J/cm<sup>2</sup> of red light. Scale bar: 100  $\mu$ m. (D) Spheroid survival evaluation was performed through Acridine Orange/Propidium Iodide staining; alive cells are fluorescing in green due to Acridine Orange, whereas death cells are fluorescing in red due to Propidium Iodide. (\*:  $p < 0.05$ ; \*\*:  $p < 0.01$ ; \*\*\*:  $p < 0.001$ ) ( $n = 3$ ). (For interpretation of the references to colour in this figure legend, the reader is referred to the web version of this article.)

major concern due to the elevated costs derived from the treatments it requires [1]. Two principal issues that these types of carcinomas present are: (1) the need for aesthetic results after treatment, since they develop in cosmetically sensitive areas like the face, neck, or other photo exposed anatomical regions, and (2) the high recurrence rates after the treatments and development of new malignancies, even metastasis, especially in the case of SCC. To overcome the first mentioned issue, several non-invasive treatments are being developed and utilized, obtaining satisfactory results [2]. For the second problem, different approaches could be applied, such as to prevent recurrences through therapy combinations, and to provide second-line treatments in the situation of an unsuccessful removal of the tumor. In this sense, we have evaluated, *in vitro*, the combination of two treatments used individually in the clinic: 5FU and PDT, applying 5FU before PDT application. To achieve this objective, we used a cell line from cutaneous SCC, SCC13, and another cell line from BCC, CSZ.

Previously, Anand et al. in 2017 successfully proved that 5FU + PDT combination induced enhanced damage in A431, a vulvar SCC line, and in xenograft models [17]. Additionally, Maytin et al. in 2018 presented a bilaterally controlled trial in AK patients proving the fact that the 5FU pre-treatment administered before PDT improves AK clearance rates. They proposed two mechanisms by which the combination might act:

higher PpIX accumulation and p53 induction [18].

Encouraged by these studies, we proposed PDT as an effective second-line treatment after the absence of an adequate 5FU response in NMSC. For that, using the above-mentioned cell lines we evaluated the effect of 5FU + PDT combination. Our results suggested a synergistic effect of both treatments in SCC13, being more effective than 5FU or PDT alone (Fig. 2A and B). These results are in concordance with previous works, even using a different SCC cell line [17,28]. Moreover, we also carried the same procedure in A431 as a positive control to prove that beneficial effect was maintained. We observed that the increased damage was higher in SCC13 than in A431, showing as indicated a synergistic vs an additive effect, respectively. We consider that the SCC13 line is as a better model to develop the 5FU acquired resistance. In contrast, in CSZ the opposite trend was observed. The combination of treatments not only did not work, but also the 5FU pre-treatment blurred the effect of the PDT itself (Fig. 2C and D). Although few studies have been carried out in BCC with 5FU + PDT combination, a clinical study in 2003 performed by Zimmermann et al. in 2003 [19] using human prostate LNCaP and human breast cancer MCF-7 cells did not obtain positive results with that combination, agreeing with the results obtained in monolayer culture of CSZ cells.

In addition, we induced 5FU resistance in SCC13 and in CSZ through



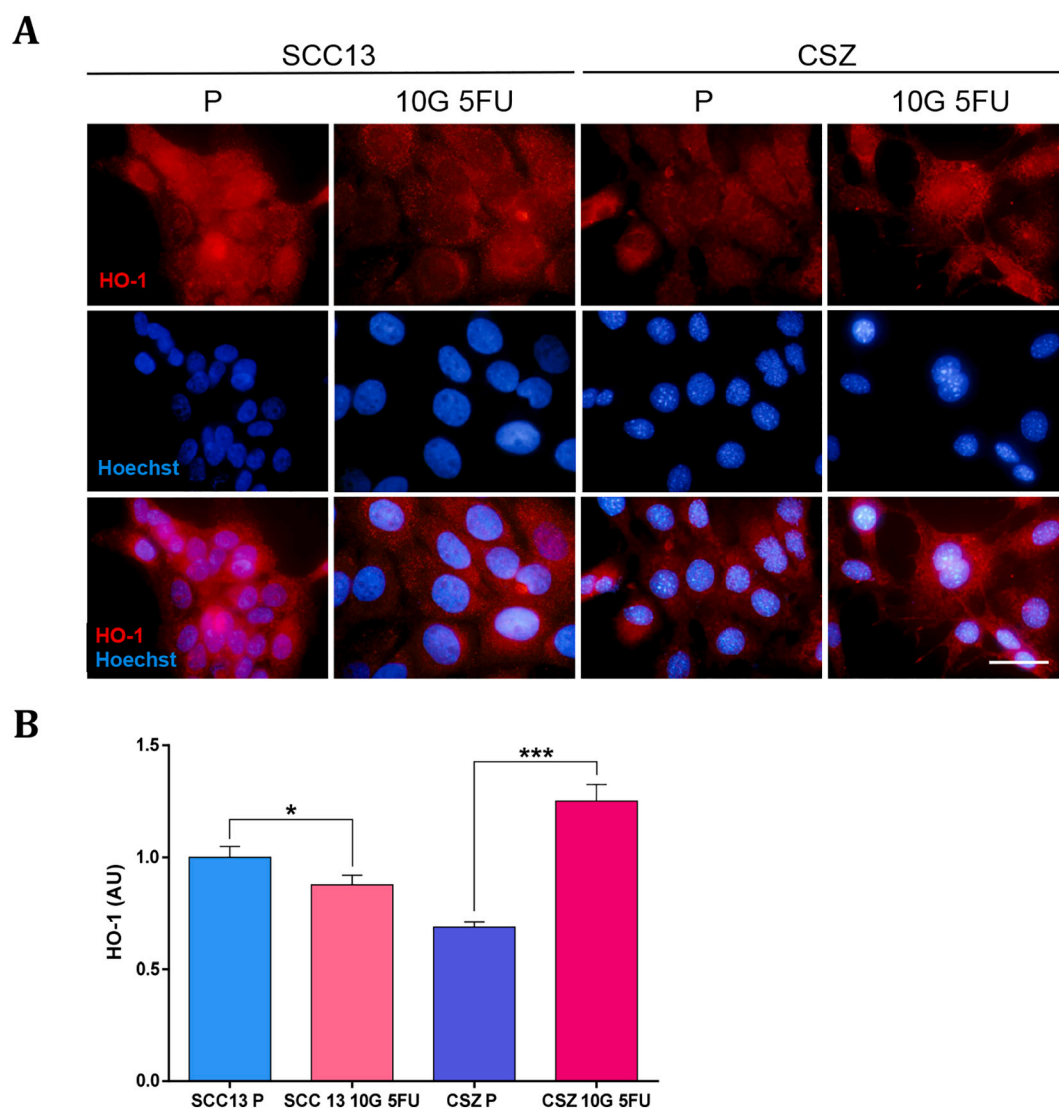


**Fig. 7. Expression of HO-1.** (A) Indirect IF of HO-1, where the red signal represents HO-1 within the cells and blue signal represent nuclei staining through Hoechst. Photographs were taken with a CCD DP70 Olympus camera. Scale bar 50  $\mu$ m. (B) Comparison analysis of HO-1 intensity signal in the different cell lines, normalized to SCC13 P (\*:  $p < 0.05$ ; \*\*:  $p < 0.01$ ; \*\*\*:  $p < 0.001$ ) ( $n = 3$ ). (For interpretation of the references to colour in this figure legend, the reader is referred to the web version of this article.)

10 cycles of 72 h treatment with this drug at 10  $\mu$ M concentration, checking the resistance of the obtained populations (see Fig. 3A). We detected that resistant cells showed a slowing down of the growth in the cultures, compared to the parental cells, evaluated by analysing the MI. This slow-down in cell proliferation has been described in other 5FU resistant lines, such as the oesophageal SCC cell line Eca-109/5-FU [14]. Besides, the CSZ 10G 5FU line displayed a morphology which resembles a mesenchymal type rather than an epithelial one, as previous authors have observed [29,30]. Anyway, further research investigating EMT makers should be evaluated in the near future.

To investigate the sensitivity to PDT, we measured the PpIX production in the four cell lines (SCC and BCC parental and resistant cell lines) by flow cytometry after MAL incubation. PpIX levels correlated with the differential sensitivity to PDT of the 5FU resistant lines compared to their parental lines (Figs. 4A and 6), as other authors have previously observed [31,32]. Therefore, we suggested that 5FU resistance promoted the accumulation of PpIX after MAL incubation, which is directly correlated with the increase in the PDT efficacy in BCC cells.

After red-light irradiation, PpIX triggers the production of ROS, determined by fluorescent microscopy, which increased in the most PDT

sensitive lines (Figs. 5 and 6). ROS production is strictly correlated with the levels of accumulated PpIX as it has previously been described [33]. Therefore, we can conclude that the higher PpIX accumulation after MAL incubation on SCC13 10G 5FU leads to a higher accumulation of ROS producing a better response to PDT. On the contrary, a decrease in PpIX accumulation and in the production of ROS within CSZ 10G 5FU results in a poorer response to PDT. We have observed an increased accumulation of PpIX in the perinuclear area in CSZ 10G 5FU compared to the parental cells that could be related to a cytoprotective autophagy process according to the suggestion indicated by Martins et al. [34]. However, studies about the subjacent molecular mechanisms involved in this response and the perinuclear PpIX accumulation are necessary.

We also evaluated the combined effect of PDT in a more complex 3D spheroids model. As expected, the trends in PDT resistance were the same as in 2D trials (Fig. 6 C and D), enforcing even more the results obtained in monolayer. The spheroids represent a better approximation to *in vivo* models regarding drug resistance, mimicking solid tumor structures and functionalities [35].

An important factor related to the response to PDT is HO-1 expression, an antioxidant molecule. The activation of antioxidant enzymes is

a manner to relieve the oxidative burden. We have observed that HO-1 is located in the nucleus of SCC13 P and CSZ 10G 5FU (Fig. 7A). This result could be related to the resistance to PDT since some authors have indicated that nuclear HO-1 promoted the expression of antioxidant factors, including Nrf2, SOD [36] and GSH among others, as well as the expression of ABCG2 [37]. In addition, HO-1 levels have been related to a differential response to PDT in different types of carcinoma cell lines [38,39]. In addition, we have observed that HO-1 levels were lower in SCC13 10G 5FU and CSZ P (Fig. 7B), which were more sensitive to PDT than SCC13 P and CSZ 10G 5FU, respectively. These results suggest that basal levels and location of HO-1 might influence the production of other antioxidant molecules as indicated before, modulating the response to PDT [37]. Additional studies considering other antioxidant molecules would be required to decipher the subjacent molecular mechanisms.

In this study two trends have been observed, while the SCC 5FU resistant cell line displayed a marked sensitivity to PDT, the BCC 5FU resistant cell line did not. These two opposite tendencies are in concordance with those obtained when applying 5FU + PDT combination on parental lines and with previous bibliography [17,19,28], where different cell lines were used but within the same type of NMSC. In recent years, several studies have confirmed the existence of crossed resistance between different treatments. For instance, in 5FU resistant colon cancer cell lines a promotion in EMT features, HES-1 and ABC transporters like ABCG2 was observed. Several efflux transporters such ABCG2, PPET1 and PEPT2 are involved in the cellular expulsion of the PS, helping to relieve the oxidative burden [15,40,41]. All these molecules are postulated as potential candidates for further studies about the mechanisms involved in the PDT response in 5FU resistant cells.

To conclude, our results indicate that the application of PDT after 5FU administration could be appropriate in SCC, but not in BCC. This strategy is also adequate for resistant tumor lesions to 5FU, so we postulate that the application of the PDT after the development of a 5FU resistance may be a good approach to take into consideration in clinical practice.

## Funding

This research was supported by Spanish grants from Instituto de Salud Carlos III Ministerio de Ciencia e innovación, and Feder Funds (FIS PI18/00708, PI21/00315 and PI21/00953).

## CRediT authorship contribution statement

**Jimena Nicolás-Morala:** Investigation, Formal analysis, Data curation, Writing – original draft, Writing – review & editing. **Mikel Portillo-Esnaola:** Investigation, Formal analysis, Data curation, Writing – original draft, Writing – review & editing. **Samuel Terrén:** Writing – review & editing. **María Gutierrez-Pérez:** Writing – review & editing. **Yolanda Gilaberte:** Conceptualization, Supervision, Funding acquisition. **Salvador González:** Conceptualization, Supervision. **Ángeles Juarranz:** Conceptualization, Supervision, Funding acquisition.

## Declaration of Competing Interest

The authors declare no conflict of interest. The funders had no role in study design; data collection, analyses, or interpretation; manuscript writing; or in the decision of the publication of results.

## Acknowledgments

Nicolás-Morala was also supported by the grants "Beca Fomento a la Investigación" from Universidad Autónoma de Madrid and "Beca Formación de Profesorado Universitario 2019" from Ministerio de Universidades. Portillo-Esnaola was also supported by "Contratos Garantía Juvenil" from Consejería de Educación e Investigación de la Comunidad

de Madrid, Spain. We also want to acknowledge Marta Mascaraque for helping in the discussion of the manuscript.

## Appendix A. Supplementary data

Supplementary data to this article can be found online at <https://doi.org/10.1016/j.jphotobiol.2022.112483>.

## References

- [1] Z. Apalla, D. Nashan, R.B. Weller, X. Castellsagué, Skin cancer: epidemiology, disease burden, pathophysiology, diagnosis, and therapeutic approaches, *Dermatol. Ther.* 7 (1) (2017) 5–19.
- [2] A. Fahradyan, A.C. Howell, E.M. Wolfswinkel, M. Tsuchi, P. Sheth, A.K. Wong, Updates on the management of non-melanoma skin cancer (NMSC). In *Healthcare* (Vol. 5, No. 4, p. 82). Multidisciplinary Digital Publishing Institute, 2017, December.
- [3] G.T. Prince, M.C. Cameron, R. Fathi, T. Alkousakis, Topical 5-fluorouracil in dermatologic disease, *Int. J. Dermatol.* 57 (10) (2018) 1259–1264.
- [4] P. Alvarez, J.A. Marchal, H. Boulaiz, E. Carrillo, C. Vélez, F. Rodríguez-Serrano, A. Aranega, 5-Fluorouracil derivatives: a patent review, *Exp. Opin. Therap. Patents* 22 (2) (2012) 107–123.
- [5] R. Gutzmer, S. Wiegand, O. Kölbl, K. Wermker, M. Heppt, C. Berking, Actinic keratosis and cutaneous squamous cell carcinoma: treatment options, *Dtsch. Arztebl. Int.* 116 (37) (2019) 616.
- [6] J. Lanoue, G. Goldenberg, Basal cell carcinoma: a comprehensive review of existing and emerging nonsurgical therapies, *J. Clin. Aesthetic Dermatol.* 9 (5) (2016) 26.
- [7] P. Agostinis, K. Berg, K.A. Cengel, T.H. Foster, A.W. Girotti, S.O. Gollnick, J. Golab, Photodynamic therapy of cancer: an update, *CA Cancer J. Clin.* 61 (4) (2011) 250–281.
- [8] A.T. Gomes, M.G. Neves, J.A. Cavaleiro, Cancer, photodynamic therapy and porphyrin-type derivatives, *An. Acad. Bras. Cienc.* 90 (1) (2018) 993–1026.
- [9] A. Casas, Clinical uses of 5-aminolevulinic acid in photodynamic treatment and photodetection of cancer: a review, *Cancer Lett.* 490 (2020) 165–173.
- [10] Y. Ohgari, Y. Nakayasu, S. Kitajima, M. Sawamoto, H. Mori, O. Shimokawa, S. Taketani, Mechanisms involved in  $\delta$ -aminolevulinic acid (ALA)-induced photosensitivity of tumor cells: relation of ferrochelatase and uptake of ALA to the accumulation of protoporphyrin, *Biochem. Pharmacol.* 71 (1–2) (2005) 42–49.
- [11] J. Cabete, M. Rafael, M. Cravo, C. Moura, F. Sachse, M. Peçegueiro, Long-term recurrence of nonmelanoma skin cancer after topical methylaminolevulinate photodynamic therapy in a dermatology-oncology department, *An. Bras. Dermatol.* 90 (2015) 846–850.
- [12] C.A. Morton, R.M. Szeimies, N. Basset-Seguín, P. Calzavara-Pinton, Y. Gilaberte, M. Haedersdal, L.R. Braathen, European dermatology forum guidelines on topical photodynamic therapy 2019 part 1: treatment delivery and established indications-actinic keratoses, Bowen's disease and basal cell carcinomas, *J. Eur. Acad. Dermatol. Venereol.* 33 (12) (2019) 2225–2238.
- [13] C. Morton, M. Horn, J. Leman, B. Tack, C. Bedane, M. Tjioe, P. Wolf, Comparison of topical methyl aminolevulinate photodynamic therapy with cryotherapy or fluorouracil for treatment of squamous cell carcinoma in situ: results of a multicenter randomized trial, *Arch. Dermatol.* 142 (6) (2006) 729–735.
- [14] C. Zhang, Q. Ma, Y. Shi, X. Li, M. Wang, J. Wang, H. Jiang, A novel 5-fluorouracil-resistant human esophageal squamous cell carcinoma cell line Eca-109/5-FU with significant drug resistance-related characteristics, *Oncol. Rep.* 37 (5) (2017) 2942–2954.
- [15] L. Sun, J. Ke, Z. He, Z. Chen, Q. Huang, W. Ai, C. Hong, HES1 promotes colorectal cancer cell resistance to 5-Fu by inducing of EMT and ABC transporter proteins, *J. Cancer* 8 (14) (2017) 2802.
- [16] S.R. Lucena, N. Salazar, T. Gracia-Cazaña, A. Zamarrón, S. González, Á. Juarranz, Y. Gilaberte, Combined treatments with photodynamic therapy for non-melanoma skin cancer, *Int. J. Mol. Sci.* 16 (10) (2015) 25912–25933.
- [17] S. Anand, K.R. Rollakanti, N. Brankov, D.E. Brash, T. Hasan, E.V. Maytin, Fluorouracil enhances photodynamic therapy of squamous cell carcinoma via a p53-independent mechanism that increases protoporphyrin IX levels and tumor cell death, *Mol. Cancer Ther.* 16 (6) (2017) 1092–1101.
- [18] E.V. Maytin, S. Anand, M. Riha, S. Lohser, A. Tellez, R. Ishak, A. Vidimos, 5-fluorouracil enhances protoporphyrin IX accumulation and lesion clearance during photodynamic therapy of actinic keratoses: a mechanism-based clinical trial, *Clin. Cancer Res.* 24 (13) (2018) 3026–3035.
- [19] A. Zimmermann, H. Walt, U. Haller, P. Baas, S.D. Klein, Effects of chlorin-mediated photodynamic therapy combined with fluoropyrimidines in vitro and in a patient, *Cancer Chemother. Pharmacol.* 51 (2) (2003) 147–154.
- [20] J.G. Rheinwald, M.A. Beckett, Tumorigenic keratinocyte lines requiring anchorage and fibroblast support cultured from human squamous cell carcinomas, *Cancer Res.* 41 (5) (1981) 1657–1663.
- [21] P.L. So, A.W. Langston, N. Daniellina, J.L. Hebert, M.A. Fujimoto, Y. Khaimskiy, E. H. Epstein Jr., Long-term establishment, characterization and manipulation of cell lines from mouse basal cell carcinoma tumors, *Exp. Dermatol.* 15 (9) (2006) 742–750.
- [22] M. Gallego-Rentero, M. Gutiérrez-Pérez, M. Fernández-Guarino, M. Mascaraque, M. Portillo-Esnaola, Y. Gilaberte, Á. Juarranz, TGF $\beta$ 1 secreted by cancer-associated fibroblasts as an inducer of resistance to photodynamic therapy in squamous cell carcinoma cells, *Cancers* 13 (22) (2021) 5613.

- [23] S.R. Lucena, A. Zamarrón, E. Carrasco, M.A. Marigil, M. Mascaraque, M. Fernández-Guarino, A. Juarranz, Characterisation of resistance mechanisms developed by basal cell carcinoma cells in response to repeated cycles of photodynamic therapy, *Sci. Rep.* 9 (1) (2019) 1–15.
- [24] G. Adhikary, D. Grun, C. Kerr, S. Balasubramanian, E.A. Rorke, M. Vemuri, R. L. Eckert, Identification of a population of epidermal squamous cell carcinoma cells with enhanced potential for tumor formation, *PLoS One* 8 (12) (2013), e84324.
- [25] T.L. Riss, R.A. Moravec, A.L. Niles, S. Duellman, H.A. Benink, T.J. Worzella, L. Minor, Cell viability assays, in: *Assay Guidance Manual* [Internet], 2016.
- [26] C.E. Olsen, K. Berg, P.K. Selbo, A. Weyergang, Circumvention of resistance to photodynamic therapy in doxorubicin-resistant sarcoma by photochemical internalization of gelonin, *Free Radic. Biol. Med.* 65 (2013) 1300–1309.
- [27] J.A. Araujo, M. Zhang, F. Yin, Heme oxygenase-1, oxidation, inflammation, and atherosclerosis, *Front. Pharmacol.* 3 (2012) 119.
- [28] L. Zhang, Z. Ji, J. Zhang, S. Yang, Photodynamic therapy enhances skin cancer chemotherapy effects through autophagy regulation, *Photodiagn. Photodyn. Ther.* 28 (2019) 159–165.
- [29] E. Galle, B. Thienpont, S. Cappuyns, T. Venken, P. Busschaert, M. Van Haele, D. Lambrechts, DNA methylation-driven EMT is a common mechanism of resistance to various therapeutic agents in cancer, *Clin. Epigenetics* 12 (1) (2020) 1–19.
- [30] B. Wang, N. Ma, X. Zheng, X. Li, X. Ma, J. Hu, B. Cao, GDF15 repression contributes to 5-fluorouracil resistance in human colon cancer by regulating epithelial-mesenchymal transition and apoptosis, *Biomed. Res. Int.* (2020) 2020.
- [31] Y. Hagiya, H. Fukuhara, K. Matsumoto, Y. Endo, M. Nakajima, T. Tanaka, S. I. Ogura, Expression levels of PEPT1 and ABCG2 play key roles in 5-aminolevulinic acid (ALA)-induced tumor-specific protoporphyrin IX (PpIX) accumulation in bladder cancer, *Photodiagn. Photodyn. Ther.* 10 (3) (2013) 288–295.
- [32] S. Yamamoto, H. Fukuhara, H. Seki, C. Kawada, T. Nakayama, T. Karashima, K. Inoue, Predictors of therapeutic efficacy of 5-aminolevulinic acid-based photodynamic therapy in human prostate cancer, *Photodiagn. Photodyn. Ther.* 35 (2021), 102452.
- [33] D. León, K. Buchegger, R. Silva, I. Riquelme, T. Viscarra, B. Mora-Lagos, P. Brebi, Epigallocatechin gallate enhances MAL-PDT cytotoxic effect on PDT-resistant skin cancer squamous cells, *Int. J. Mol. Sci.* 21 (9) (2020) 3327.
- [34] W.K. Martins, R. Belotto, M.N. Silva, D. Grasso, M.D. Suriani, T.S. Lavor, T. M. Tsubone, Autophagy regulation and photodynamic therapy: insights to improve outcomes of cancer treatment, *Front. Oncol.* 11 (2021) 3121.
- [35] A.S. Nunes, A.S. Barros, E.C. Costa, A.F. Moreira, L.J. Correia, 3D tumor spheroids as in vitro models to mimic in vivo human solid tumors resistance to therapeutic drugs, *Biotechnol. Bioeng.* 116 (1) (2019) 206–226.
- [36] C. Biswas, N. Shah, M. Muthu, P. La, A.P. Fernando, S. Sengupta, P.A. Dennerly, Nuclear heme oxygenase-1 (HO-1) modulates subcellular distribution and activation of Nrf2, impacting metabolic and anti-oxidant defenses, *J. Biol. Chem.* 289 (39) (2014) 26882–26894.
- [37] C. Donohoe, M.O. Senge, L.G. Arnaut, L.C. Gomes-da-Silva, Cell death in photodynamic therapy: from oxidative stress to anti-tumor immunity, *Biochim. Biophys. Acta (BBA)-Rev. Cancer* 1872 (2) (2019), 188308.
- [38] D. Nowis, M. Legat, T. Grzela, J. Niderla, E. Wilczek, G.M. Wilczynski, J. Gołab, Heme oxygenase-1 protects tumor cells against photodynamic therapy-mediated cytotoxicity, *Oncogene* 25 (24) (2006) 3365–3374.
- [39] M. Mastrangelopoulou, M. Grigalavicius, T.H. Raabe, E. Skarpen, P. Juzenas, Q. Peng, T.A. Theodossiou, Predictive biomarkers for 5-ALA-PDT can lead to personalized treatments and overcome tumor-specific resistances, *Cancer Rep.* e1278 (2020).
- [40] Y. Hagiya, Y. Endo, Y. Yonemura, K. Takahashi, M. Ishizuka, F. Abe, S.I. Ogura, Pivotal roles of peptide transporter PEPT1 and ATP-binding cassette (ABC) transporter ABCG2 in 5-aminolevulinic acid (ALA)-based photocytotoxicity of gastric cancer cells in vitro, *Photodiagn. Photodyn. Ther.* 9 (3) (2012) 204–214.
- [41] N. Kawai, Y. Hirohashi, Y. Ebihara, T. Saito, A. Murai, T. Saito, T. Torigoe, ABCG2 expression is related to low 5-ALA photodynamic diagnosis (PDD) efficacy and cancer stem cell phenotype, and suppression of ABCG2 improves the efficacy of PDD, *PLoS One* 14 (5) (2019), e0216503.